

# ASYMPTOTIC CALCULATION OF FREE CONVECTION IN LAMINAR THREE-DIMENSIONAL SYSTEMS

WARREN E. STEWART

Chemical Engineering Department, University of Wisconsin, Madison, Wisconsin, U.S.A.

(Received 23 January 1970)

**Abstract**—Boundary-layer solutions are given for free convection in laminar three-dimensional systems, driven by a temperature-dependent or composition-dependent density. Effects of rapid mass transfer and centrifugal forces are determined, and the results of Acrivos [1] for power-law fluids are generalized. The results hold asymptotically for large Prandtl or Schmidt number; they are strikingly confirmed by previous measurements of diffusion-limited electrochemical reactions.

## INTRODUCTION

THE EFFECTS of surface shape and orientation on free convection are important in heat transfer, drying, and electrode processes. These effects are difficult to calculate exactly; however, at moderately large Prandtl or Schmidt numbers, they are tractable by boundary-layer methods. Acrivos [1] used this approach to calculate free-convection heat transfer in two-dimensional and axially symmetric geometries. Here this approach is generalized to three-dimensional systems, centrifugal fields and high mass-transfer rates.

## NOMENCLATURE

For each physical quantity, the dimensions are given in terms of mass ( $m$ ), length ( $l$ ) and temperature ( $T$ ).

$A$ , area of transfer surface [ $l^2$ ];  
 $a$ , linear acceleration of reference point [ $lt^{-2}$ ];  
 $B$ , vector stream function in equation (19) [dimensionless];  
 $\bar{C}_p$ , mean heat capacity of inner layer [ $l^2t^{-2}T^{-1}$ ];  
 $D$ , diameter of cylinder or sphere [ $l$ ];  
 $\mathcal{D}_{AB}$ , mean binary diffusivity of inner layer [ $l^2t^{-1}$ ];

$F_D$ , vertical drag force on solid; positive upward [ $mlt^{-2}$ ];  
 $f$ , reduced stream function, defined in equation (31) [dimensionless];  
 $f', f'', f'''$ , derivatives of  $f$  with respect to  $\eta$  [dimensionless];  
 $f''(0)$ , interfacial value of  $d^2f/d\eta^2$  [dimensionless];  
 $G$ , potential energy gradient, equations (17) and (76) [dimensionless];  
 $Gr$ , thermal Grashof number, equation (59) [dimensionless];  
 $Gr_\omega$ , diffusional Grashof number, from equations (59) and (77) [dimensionless];  
 $g$ , acceleration of gravity [ $lt^{-2}$ ];  
 $g_{eff}$ , effective local acceleration in moving coordinates [ $lt^{-2}$ ];  
 $h$ ,  $= 0.5402 k/\delta_T$ , local heat-transfer coefficient in absence of mass transfer; see equation (47) [ $mt^{-3}T^{-1}$ ];  
 $h_m$ ,  $= 0.5402 (k/l)K_2|GrPr|^{1/2}$ , mean value of  $h$ ; see equation (51) [ $mt^{-3}T^{-1}$ ];  
 $h_x, h_y, h_z$ , scale factors of equation (16) [dimensionless];  
 $j_{A0}$ , interfacial diffusion flux,  $n_{A0} - \omega_{A0}(n_{A0} + n_{B0})$  [ $ml^{-2}t^{-1}$ ];

$K$ , coefficient in power law, equation (57) [ $ml^{-1}t^{n-2}$ ];

$K_1, K_2$ , coefficients in equations (49) and (51) [dimensionless];

$k$ , mean thermal conductivity of inner layer [ $mlt^{-3}T^{-1}$ ];

$k_\omega$ , = 0.5402  $\rho \mathcal{D}_{AB}/\delta_\omega$ , local mass-transfer coefficient at small net mass flux; see equations (47) and (77) [ $ml^{-2}t^{-1}$ ];

$k_{\omega m}$ , = 0.5402  $(\rho \mathcal{D}_{AB}/l) K_2 |Gr_\omega Sc|^\frac{1}{4}$ , mean value of  $k_\omega$ ; see equations (51) and (77) [ $ml^{-2}t^{-1}$ ];

$l$ , characteristic length of transfer surface [ $l$ ];

$Nu_m$ , =  $Ql/Ak(T_0 - T_\infty)$ , mean thermal Nusselt number at prevailing mass-transfer rate [dimensionless];

$Nu_{\omega m}$ , =  $[w_{A0} - \omega_{A0}(w_{A0} + w_{B0})]/A\rho \mathcal{D}_{AB}(\omega_{A0} - \omega_{A\infty})$ , mean diffusional Nusselt number at prevailing mass-transfer rate [dimensionless];

$n$ , exponent in power law, equation (57), unity for Newtonian flow [dimensionless];

$n_{A0}, n_{B0}$ , local mass fluxes of species  $A$  and  $B$  into fluid at  $y = 0$ , relative to the solid surface [ $ml^{-2}t^{-1}$ ];

$\mathcal{P}$ , hydrostatic function,  $p + \rho_\alpha \hat{\Phi}$  [ $ml^{-1}t^{-2}$ ];

$p$ , static pressure [ $ml^{-1}t^{-2}$ ];

$Pr$ , Prandtl number, equation (60) [dimensionless];

$Q$ , total rate of heat transfer into fluid by conduction at interface  $y = 0$  [ $ml^2t^{-3}$ ];

$q_0$ , conductive heat flux into fluid at  $y = 0$  [ $mt^{-3}$ ];

$R$ , flux ratio,  $R_T$  or  $R_\omega$  [dimensionless];

$R_T$ , thermal flux ratio in equation (52) [dimensionless];

$R_\omega$ , =  $(\omega_{A0} - \omega_{A\infty}) / \left[ \frac{n_{A0}}{n_{A0} + n_{B0}} - \omega_{A0} \right]$ ,

mass flux ratio [dimensionless];

position vector [ $l$ ];

$Sc$ , Schmidt number, from equations (60) and (77) [dimensionless];

$T$ , temperature;

$\mathbf{v}^*$ , velocity vector [ $lt^{-1}$ ];

$\mathbf{v}$ , dimensionless velocity vector,  $\mathbf{v}^*/\alpha$  or  $\mathbf{v}^*/\mathcal{D}_{AB}$ ;

$\mathbf{v}^{(i)}$ , inner approximation to  $\mathbf{v}$ ;

$w_{A0}, w_{B0}$ , total rates of mass transfer of species  $A$  and  $B$  into fluid [ $mt^{-1}$ ];

$x, y, z$ , boundary-layer coordinates [dimensionless];

$x_s(z)$ , starting (stagnation) locus for flow over transfer surface;

$x_f(z)$ , finishing locus for flow over transfer surface;

$y^*$ , =  $yl$ , actual distance from nearest point of surface [ $l$ ];

$z_I, z_{II}$ , lower and upper limits of  $z$  for transfer surface.

Greek symbols

$\alpha$ , =  $k/\rho \hat{C}_p$ , thermal diffusivity [ $l^2t^{-1}$ ];

$\beta_T$ , thermal expansion coefficient,  $(-\partial \ln \rho/\partial T)_p$  at mean temperature of inner layer [ $T^{-1}$ ];

$\beta_{\omega A}$ , binary expansion coefficient,  $(-\partial \ln \rho/\partial \omega_A)_p$  at mean composition of inner layer [dimensionless];

$\gamma$ , angle of inclination of cylinder (Fig. 4) [dimensionless];

$\delta, \delta_T, \delta_\omega$ , characteristic boundary-layer thicknesses based on velocity, temperature, and composition [ $l$ ];

$\delta_i$ , unit vector in the direction of coordinate  $i$  [dimensionless];

$\zeta$ , axial polar coordinate relative to  $D$  in Fig. 4 [dimensionless];

$\eta$ , similarity coordinate in equation (33) or its binary analog [dimensionless];

$\Theta$ , dimensionless temperature,  $(T - T_\infty)/(T_0 - T_\infty)$  or composition,  $(\omega_A - \omega_{A\infty})/(\omega_{A0} - \omega_{A\infty})$ ;

$\Theta', \Theta''$ , derivatives of  $\Theta$  with respect to  $\eta$  [dimensionless];  
 $\Theta'(0)$ , interfacial value of  $d\Theta/d\eta$  [dimensionless];  
 $\nu$ , mean kinematic viscosity of inner layer [ $l^2 t^{-1}$ ];  
 $\xi$ , radial coordinate relative to D in cylindrical or spherical coordinates;  
 $\rho$ , mean density of inner layer [ $ml^{-3}$ ];  
 $\rho_\infty$ , density of fluid outside boundary layer [ $ml^{-3}$ ];  
 $\tau_{yx}$ , flux of tangential momentum in  $y$  direction [ $ml^{-1}t^{-2}$ ];  
 $\tau_0$ , interfacial shear stress on solid,  $-\tau_{yx}|_{y=0}$  [ $ml^{-1}t^{-2}$ ];  
 $\hat{\Phi}$ , potential energy, [ $l^2 t^{-2}$ ];  
 $\phi$ , dimensionless mass flux,  $\phi_T$  or  $\phi_\omega$ ;  
 $\phi_T$ , dimensionless mass flux for heat transfer, equation (56);  
 $\phi_\omega$ , dimensionless mass flux for binary diffusion,  $(n_{A0} + n_{B0})/k_\omega = (w_{A0} + w_{B0})/k_{om}A$ ;  
 $\varphi$ , function defined in equation (31) [dimensionless];  
 $\psi$ , stream function defined in equations (20)–(22) [dimensionless];  
 $\omega$ , angular velocity of rotating system;  
 $\omega_A$ , mass fraction of species A.

**Subscripts**

A, B, chemical species;  
 $s, f$ , starting, finishing;  
 $T, \omega$ , thermal, diffusional;  
 $t$ , tangential (projection on tangent plane at nearest surface point);  
 $x, y, z$ , coordinate directions;  
 $0$ , at  $y = 0$ ;  
 $\infty$ , at  $y = \infty$ ;  
 $1$ , dummy variable.

**Superscripts**

( $i$ ), inner solution;  
 $\sim$ , per unit mass;  
 $*$ , dimensional.

**Operations**

$\nabla$ , Del operator in space with all lengths divided by  $l$  [dimensionless];  
 $\nabla^s$ , projection of operator  $\nabla$  onto the transfer surface;  
 $(0)$ , evaluated at  $\eta = 0$ ;  
 $abs$ , absolute value.

**BASIC EQUATIONS**

Consider the transfer of heat from a solid surface to a pure fluid, by steady, laminar free convection. The rates of momentum and heat transfer between the solid and fluid are to be calculated. If the surface is smooth and free of pockets which would tend to fill with heated fluid, then the following boundary-layer equations are accurate for  $|GrPr| \gg 1$ :

*Continuity:*

$$(\nabla \cdot \mathbf{v}) = 0 \tag{1}$$

*Motion (tangential):*

$$\frac{1}{Pr^2} [\mathbf{v} \cdot \nabla \mathbf{v}]_t = \frac{1}{Pr} \frac{\partial^2 \mathbf{v}_t}{\partial y^2} - \frac{\mathbf{g}_t}{g} Gr\Theta \tag{2}$$

*Motion (normal):*

$$\frac{1}{Pr^2} \frac{\partial}{\partial y} (p + \rho_\infty \hat{\Phi}) \frac{l^2}{\rho \alpha^2} = - \frac{g_y}{g} Gr\Theta \tag{3}$$

*Energy:*

$$(\mathbf{v} \cdot \nabla \Theta) = \frac{\partial^2 \Theta}{\partial y^2}. \tag{4}$$

Here the physical properties are considered constant, except that the thermal buoyant force is included. The coordinates and velocity are dimensionless relative to  $l$  and  $\alpha/l$ , where  $\alpha$  is the thermal diffusivity and  $l$  is a characteristic length of the surface. The coordinate  $y$  is the dimensionless distance from the surface into the fluid, and  $\Theta$  is a dimensionless temperature (see Nomenclature). The Grashof number,  $Gr$ , is positive when the buoyant force is upward.

We wish to determine the rates of heat and momentum transfer at the surface, under the following boundary conditions:

$$\text{at } y = 0: \quad v_t = 0, \quad \Theta = 1, \quad v_y = 0 \quad (5, 6, 7)$$

$$\text{at } y/\delta \rightarrow \infty: \quad v_t \rightarrow 0, \quad \Theta \rightarrow 0,$$

$$p + \rho_\infty \Phi \rightarrow \mathcal{P}_\infty = \text{const.} \quad (8, 9, 10)$$

Equation (5) is the no-slip condition. Equation (7) is the condition of no mass transfer, and will be relaxed later. Equation (10) is the condition of hydrostatic equilibrium outside the boundary layer. These conditions hold over the heat transfer region, which extends from  $x_s(z)$  to  $x_f(z)$  and from  $z_1$  to  $z_{II}$  in the surface coordinates  $(x, z)$  (see Fig. 1). In addition, the following condition is given at the upstream boundary of the transfer region:

$$\text{at } x = x_s(z), \quad v_t = 0 \quad \text{for all } y. \quad (11)$$

This means that the upstream boundary is always a stagnation locus, whatever the surface geometry may be. This condition is required by the boundary-layer approximations made in equations (2) and (4), which permit no tangential transmission of heat or momentum except by convection downstream. We do not prescribe the fluid temperature at  $x = x_s(z)$ , since an adiabatic condition across this surface is implied by equations (4) and (11).

The pressure can be determined readily from equations (3) and (10):

$$(p + \rho_\infty \Phi - \mathcal{P}_\infty) \frac{l^2}{\rho \alpha^2} = \frac{g_y}{g} Gr Pr^2 \int_y^\infty \Theta dy. \quad (12)$$

This variation in  $(p + \rho_\infty \Phi)$  is negligible in the tangential equation of motion, but it is significant in determining the drag force on the solid.

#### SIMPLIFICATION FOR LARGE $Pr$

At large Prandtl numbers, on surfaces free of pockets or level planes, the thermal boundary layer becomes very thin and the flow becomes very slow. Equation (2) then reduces to

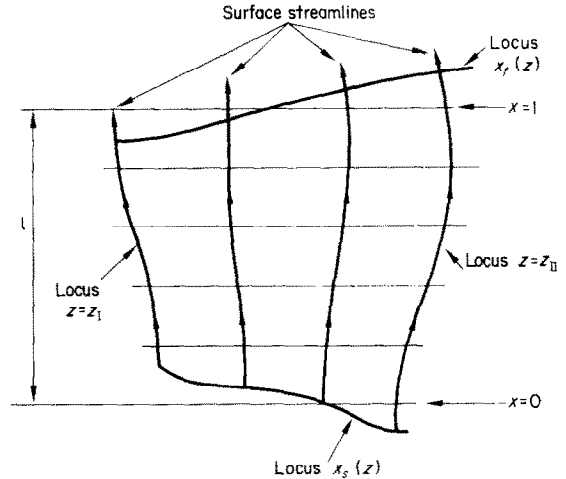


FIG. 1. Surface coordinates for a transfer region on a three-dimensional body with upward flow (positive  $Gr$ ). For downward flow boundaries  $x_s(z)$  and  $x_f(z)$  would be interchanged.

$$\frac{\partial^2 v_t^{(i)}}{\partial y^2} = \frac{g_t}{g} Gr Pr \Theta \quad (13)$$

wherever  $g_t$  and  $\Theta$  are non-zero. The velocity  $v^{(i)}$  thus described is an "inner solution", accurate in the thermal boundary layer, and subject to the following boundary condition in place of equation (8):

$$\text{at } y/\delta_T \rightarrow \infty: \quad \frac{\partial v_t^{(i)}}{\partial y} \rightarrow 0. \quad (14)$$

This boundary condition is required in order that  $v^{(i)}$  remain finite at large  $y$ , in keeping with the matching requirements of singular perturbation theory [2]. It is also physically appropriate, since at large Prandtl numbers the true tangential velocity attains its peak near the edge of the thermal layer (see Fig. 2), where  $y/\delta_T$  is large, while  $y/\delta$  is still small [3].

With these changes, the boundary-layer problem is reduced to a description of the thermal layer at large  $Pr$ . The flow outside this inner layer will not be considered here. The transfer rates thus calculated are exact in the limit of large  $Pr$ ; this has been shown by Morgan and Warner [4] for two-dimensional systems, and

the extension of their proof to three dimensions is straightforward.

**STREAMLINES AND COORDINATES**

The tangential velocity  $v_t^{(i)}$  can be calculated formally by integrating equation (13), under the boundary conditions (5) and (14):

$$v_t^{(i)} = - (g_x/g) GrPr \int_0^y \int_{y'}^\infty \Theta(x, y'', z) dy'' dy'. \quad (15)$$

Thus the tangential velocity  $v_t^{(i)}$  is in the direction of  $g_x Gr$ , i.e. the direction of steepest ascent or descent along the adjoining surface.

To capitalize on equation (15), we take the dimensionless elevation on the surface as the coordinate  $x$ , and the steepest-descent lines as the lines of constant  $z$  (see Fig. 1). For each point in the fluid, we take  $x$  and  $z$  as the values at the nearest surface point. Then  $v_z^{(i)}$  and  $g_z$  vanish, and only the  $x$ -component of equation (13) is needed.

The coordinates  $x, y, z$  are orthogonal at the surface, and essentially so throughout the boundary layer, except where the nearest surface

point is on a sharp corner, vertex or level plane. Such exceptional regions are excluded from this treatment. The scale factors [5] for these coordinates are defined in terms of the dimensionless vector element of displacement,

$$ds = \delta_x h_x dx + \delta_y h_y dy + \delta_z h_z dz \quad (16)$$

in which  $\delta_x, \delta_y$  and  $\delta_z$  are unit vectors in the  $x, y$  and  $z$  directions. The factor  $h_y$  is unity; the other two are approximated by their values at the surface (since the boundary layer is thin):

$$h_x = \frac{1}{|\nabla^s x|} = \frac{g}{-g_x}, \text{ abbreviated } \frac{1}{G(x, z)} \quad (17)$$

$$h_z = \frac{1}{|\nabla^s z|}. \quad (18)$$

Here  $\nabla^s$  denotes the gradient taken along the surface. The dependence of  $h_x$  and  $h_z$  on  $x$  and  $z$  is assumed to be smooth, but otherwise arbitrary. The use of equations (16–18) is illustrated in the Appendix.

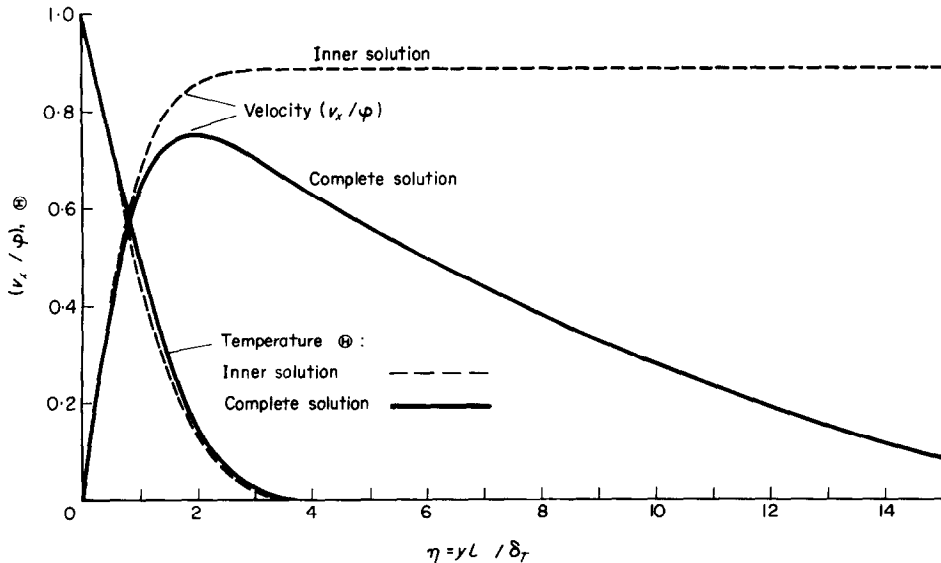


FIG. 2. Boundary-layer profiles near a heated vertical plate with  $Pr = 100$ . Solid lines are exact solutions of equations (1)–(12); dashed lines are solutions of equations (1), (3)–(7) and (9)–(14). The quantities  $\phi$  and  $\delta_T$  are calculated from equations (42) and (43) with  $h_z = 1$  and  $G = 1$ .

Equation (1) can be satisfied directly by writing  $v^{(i)}$  in the form

$$v^{(i)} = \text{curl } \mathbf{B} = \frac{1}{h_x h_y h_z} \begin{vmatrix} h_x \delta_x & h_y \delta_y & h_z \delta_z \\ \frac{\partial}{\partial x} & \frac{\partial}{\partial y} & \frac{\partial}{\partial z} \\ h_x B_x & h_y B_y & h_z B_z \end{vmatrix} \quad (19)$$

where  $B_x$ ,  $B_y$  and  $B_z$  are functions to be determined. Here we assume that the scale factors are differentiable as needed. In the present coordinates,  $v_z^{(i)}$  is zero; hence  $B_x$  and  $B_y$  can be discarded, and a single stream function,  $\psi = h_z B_z$ , is adequate. Then with  $h_y = 1$  the velocity components in the thermal layer become:

$$v_x^{(i)} = \frac{1}{h_z} \frac{\partial \psi}{\partial y};$$

$$v_y^{(i)} = -\frac{1}{h_x h_z} \frac{\partial \psi}{\partial x}; \quad v_z^{(i)} = 0. \quad (20, 21, 22)$$

Insertion of equations (16–22) into equations (13) and (4) gives:

$$\frac{1}{G h_z} \frac{\partial^3 \psi}{\partial y^3} = -GrPr\Theta \quad (23)$$

$$\frac{G}{h_z} \left( \frac{\partial \psi}{\partial y} \frac{\partial \Theta}{\partial x} - \frac{\partial \psi}{\partial x} \frac{\partial \Theta}{\partial y} \right) = \frac{\partial^2 \Theta}{\partial y^2}. \quad (24)$$

The boundary conditions on  $\psi$  and  $\Theta$  are:

$at\ y = 0:$	$\frac{\partial \psi}{\partial y} = 0,$	$\Theta = 1,$	$\psi = \text{const.}$	}	from	$x = x_s(z)$	(25, 26, 27)
$at\ y/\delta_T \rightarrow \infty:$	$\frac{\partial^2 \psi}{\partial y^2} = 0,$	$\Theta = 0$		}	to		
$at\ x = x_s(z): \psi = \text{const. for all } y > 0.$							(30)

The constant in equations (27) and (30) can be taken as zero without loss of generality.

Equations (23)–(30) contain no  $z$ -derivatives,

and can thus be solved in two dimensions at each value of  $z$ . In the next section, the problem is further reduced to one dimension.

**SOLUTION BY COMBINATION OF VARIABLES**

The form of the boundary conditions (25)–(30) suggests a combination of variables. Hence the following form of solution is tried:

$$\psi = \varphi(x, z) f(\eta) \quad (31)$$

$$\Theta = \Theta(\eta) \quad (32)$$

$$\eta = yl/\delta_T(x). \quad (33)$$

Insertion of these postulates into equations (23) and (24) gives

$$\left[ \frac{\varphi l^3}{GrPrh_z G \delta_T^3} \right] f''' = -\Theta \quad (34)$$

$$- \left[ \frac{G \delta_T}{h_z l} \frac{\partial \varphi}{\partial x} \right] f \Theta' = \Theta'' \quad (35)$$

in which  $f''' = d^3 f/d\eta^3$ ,  $\Theta'' = d^2 \Theta/d\eta^2$ , etc. Equations (25)–(29) correspondingly become:

$$at\ \eta = 0: f' = 0, \Theta = 1, f = 0 \quad (36, 37, 38)$$

$$at\ \eta = \infty: f'' = 0, \Theta = 0. \quad (39, 40)$$

Equation (30) gives, with the constant taken as zero:

$$at\ x = x_s(z): \varphi = 0. \quad (41)$$

Now, if  $f$  and  $\Theta$  are to depend only on  $\eta$ , the bracketted terms in (34) and (35) must be taken as constants. Taking them both equal to unity

leads to the following solutions for  $\varphi$  and  $\delta_T$ :

$$\Theta'' = -f\Theta' \tag{45}$$

$$\varphi = GrPr \left[ \frac{4}{3GrPr} \int_{x_1(z)}^x \frac{h_z^{\frac{4}{3}}}{G^{\frac{4}{3}}} dx \right]^{\frac{3}{2}} \tag{42}$$

$$\frac{\delta_T}{l} = (h_z G)^{-\frac{1}{2}} \left[ \frac{4}{3GrPr} \int_{x_1(z)}^x \frac{h_z^{\frac{4}{3}}}{G^{\frac{4}{3}}} dx \right]^{\frac{3}{2}} \tag{43}$$

Equations (34) and (35) then become

$$f''' = -\Theta \tag{44}$$

and the combination of variables is confirmed.

Numerical solutions of equations (44) and (45) under the boundary conditions (36)–(40) are shown in Fig. 2. Also shown are the exact profiles for a vertical plate with  $Pr = 100$ . The asymptotic calculations are closely confirmed within the thermal boundary layer.

The interfacial shear stress  $\tau_0$  and energy flux  $q_0$  are given by the dimensionless expressions

$$\frac{\tau_0}{l\rho g\beta_T(T_0 - T_\infty)} = G \frac{\delta_T}{l} \int_0^\infty \Theta d\eta = f''(0) \frac{G^{\frac{1}{2}}}{h_z^{\frac{1}{2}}} \left[ \frac{4}{3GrPr} \int_{x_1(z)}^x \frac{h_z^{\frac{4}{3}}}{G^{\frac{4}{3}}} dx \right]^{\frac{3}{2}} \tag{46}$$

and

$$\frac{q_0 l}{k(T_0 - T_\infty)} = -\Theta'(0) \frac{l}{\delta_T} = -\Theta'(0) (h_z G)^{\frac{1}{2}} \left[ \frac{4}{3GrPr} \int_{x_1(z)}^x \frac{h_z^{\frac{4}{3}}}{G^{\frac{4}{3}}} dx \right]^{-\frac{3}{2}} \tag{47}$$

Here  $q_0 l/k(T_0 - T_\infty)$  is the local Nusselt number. The values of  $f''(0)$  and  $\Theta'(0)$  for the present problem are 1.085 and  $-0.5402$ . Values for related problems will be considered below.

The vertical drag force on the solid is given by the surface integral of  $(p + \rho_\infty \hat{\Phi} - \mathcal{P}_\infty) g_y/g - \tau_{yx} g_x/g$ . Using equations (12) and (15), one obtains:

$$\frac{F_D}{l^3 \rho g \beta_T (T_0 - T_\infty)} = \int_{z_I}^{z_H} \int_0^\infty \int_{x_1(z)}^{x_f(z)} |\Theta h_x h_y h_z dx dy dz|. \tag{48}$$

Use of equations (33), (39), (43) and (44) then gives:

$$\begin{aligned} \frac{F_D}{l^3 \rho g \beta_T (T_0 - T_\infty)} &= f''(0) \int_{z_I}^{z_H} \int_{x_1(z)}^{x_f(z)} |(\delta_T/l) h_x h_z dx dz| \\ &= f''(0) |GrPr|^{-\frac{1}{2}} \text{abs} \int_{z_I}^{z_H} \int_{x_1(z)}^{x_f(z)} \left| \frac{4}{3} \int_{x_1(z)}^x G^{-\frac{4}{3}} h_z^{\frac{4}{3}} dx_1 \right|^{\frac{3}{2}} G^{-\frac{1}{2}} h_z^{\frac{4}{3}} dx dz \\ &= f''(0) |GrPr|^{-\frac{1}{2}} K_1. \end{aligned} \tag{49}$$

The integral  $K_1$  is a function of the geometry alone. Values for several systems are given in Table 1, and their determination is described in the Appendix.

The mean Nusselt number,  $Nu_m$ , is obtained by averaging equation (47) over the surface:

$$\begin{aligned}
 Nu_m \text{ abs} \int_{z_I}^{z_H} \int_{x_s(z)}^{x_f(z)} h_x h_z dx dz &= -\Theta'(0) \text{ abs} \int_{z_I}^{z_H} \int_{x_s(z)}^{x_f(z)} \frac{l}{\delta_T} h_x h_z dx dz \\
 &= -\Theta'(0) \text{ abs} \int_{z_I}^{z_H} \int_{x_s(z)}^{x_f(z)} \frac{\partial \varphi}{\partial x} dx dz \\
 &= -\Theta'(0) |GrPr|^{\frac{1}{2}} \text{ abs} \int_{z_I}^{z_H} \left| \frac{4}{3} \int_{x_s(z)}^{x_f(z)} G^{-\frac{1}{3}} h_z^{\frac{4}{3}} dx \right|^{\frac{1}{2}} dz \quad (50)
 \end{aligned}$$

or

$$Nu_m = -\Theta'(0) |GrPr|^{\frac{1}{2}} K_2. \quad (51)$$

This equation is the key result of the present paper. Calculated values of  $K_2$  are given in Table 1. Comparisons with experimental data are given in Table 2; the agreement is excellent.

Equation (50) holds for heating or cooling, and gives the same value of  $K_2$ , since reversal of the temperature difference merely interchanges the limits  $x_s(z)$  and  $x_f(z)$ . No such symmetry holds for  $K_1$  unless the transfer surface looks the same from above and below; this is illustrated by the results in Table 1.

Brenner [9] has shown that in forced convection from an isothermal surface, the Nusselt number is invariant to reversal of the velocity field. The result in equation (50) is even more surprising, because more complicated changes in the velocity profiles are involved.

#### HEAT TRANSFER WITH INTERPHASE MASS TRANSFER (PURE FLUIDS)

Suppose that a pure substance passes through the interface where the heat transfer occurs, and that the interfacial mass flux  $n_{A0}$  is proportional to  $q_0$  at all points. Examples of this are evaporation or condensation of a pure substance A at a porous surface exposed to pure superheated vapor A.

The proportionality of  $n_{A0}$  and  $q_0$  is conveni-

ently written as a thermal flux ratio,

$$\frac{n_{A0} \hat{C}_p (T_0 - T_\infty)}{q_0} = R_T = \left\{ \begin{array}{l} \text{constant for} \\ \text{all surface} \\ \text{points } (x, 0, z) \end{array} \right\} \quad (52)$$

which serves to compare the interfacial convective and conductive energy fluxes [10]. The interfacial value of  $v_y$ , now becomes  $n_{A0} l / \rho \alpha$ , and equation (7) is replaced as follows:

$$\text{at } y = 0, \quad v_y = -R_T \frac{\partial \Theta}{\partial y}. \quad (53)$$

Equation (27) then is replaced by:

$$\text{at } y = 0, \quad \frac{1}{h_x h_z} \frac{\partial \psi}{\partial x} = R_T \frac{\partial \Theta}{\partial y}. \quad (54)$$

The rest of equations (1)–(30) remain as before.

The solution in the previous section can be extended readily to this situation. Insertion of equations (31)–(33) into (54) gives

$$f(0) = R_T \Theta'(0) \quad (55)$$

in place of equation (38). Equations (44) and (45) can now be integrated, with this new boundary condition, to obtain the temperature and velocity profiles in the presence of mass transfer.

The velocity and temperature profiles, found by numerical integration, are plotted in Fig. 3.



Table 1. Geometric factors for interphase transfer

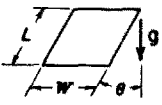
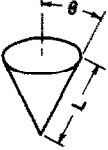
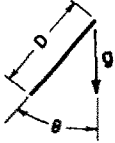
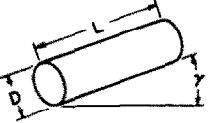
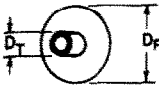
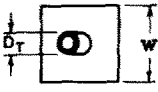
Geometry	Characteristic Length,	Other Specifications	$K_1$	$K_2$
Sphere	Diameter, $D$		3.20	1.090
Rectangular plate (one side) 	Slant Height, $L$	$\theta \neq \pi/2$	$\frac{0.860(W/L)}{(\cos \theta)^{1/4}}$	$1.241(\cos \theta)^{1/4}$
Vertical cone, base insulated 	Slant Height, $L$	Flow Toward Base, $\theta \neq \pi/2$	$\frac{2.43 \sin \theta}{(\cos \theta)^{1/4}}$	$1.314 (\cos \theta)^{1/4}$
		Flow Toward Vertex, $\theta \neq \pi/2$	$\frac{2.75 \sin \theta}{(\cos \theta)^{1/4}}$	$1.314 (\cos \theta)^{1/4}$
Inclined disk (one side) 	Diameter, $D$	$\theta \neq \pi/2$	$\frac{0.645}{(\cos \theta)^{1/4}}$	$1.305 (\cos \theta)^{1/4}$
Inclined cylinder, ends insulated 	Diameter, $D$	$Z = (L/D) \cot \gamma \rightarrow 0$	$K_1(D/L)(\cos \gamma)^{1/4} = 2.70 Z^{1/4}$	$K_2 (\cos \gamma)^{1/4} = 1.241 Z^{-1/4}$
		$Z = 0.5$	2.26	1.486
		$Z = 1.0$	2.66	1.272
		$Z = 2.0$	3.04	1.128
		$Z = \infty$	3.61	0.958
Flat surfaces of isothermal disk fin on a horizontal tube 	Fin Diameter, $D_F$	$B = (D_T/D_F) \rightarrow 0$	$K_1 = 1.29$	$K_2 = 1.30$
		0.25	1.14	1.39
		0.50	0.83	1.54
		0.75	0.41	1.81
		1.00	$2.79(1-B)^{5/4}$	$1.27(1-B)^{-1/4}$
Flat surfaces of isothermal square fin on a horizontal tube 	Fin Width, $W$	$B = (D_T/W) \rightarrow 0$	$K_1 = 1.72$	$K_2 = 1.24$
		0.25	1.56	1.31
		0.50	1.25	1.40
		0.75	0.80	1.56
		1.00	0.25	1.94

Table 2. Comparisons with electrochemical measurements

Geometry	Prediction of equation (51), derived for $Nu \gg 1$ and $Pr \gg 1$	Correlation of data for for $Nu_{\omega m} > 50$ and $Sc \sim 10^3$	Correlation references
Sphere ( $l = D$ )	$Nu_m = 0.589  Gr Pr ^{\frac{1}{2}}$	$Nu_{\omega m} = 2 + 0.59  Gr_{\omega} Sc ^{\frac{1}{2}}$	[6]
Vertical plate ( $l = \text{height}$ )	$Nu_m = 0.670  Gr Pr ^{\frac{1}{2}}$	$Nu_{\omega m} = 0.66  Gr_{\omega} Sc ^{\frac{1}{2}}$	[7, 8]
Horizontal cylinder ( $l = D$ )	$Nu_m = 0.518  Gr Pr ^{\frac{1}{2}}$	$Nu_{\omega m} = 0.53  Gr_{\omega} Sc ^{\frac{1}{2}}$	[6]

at various mass-transfer rates as measured by the dimensionless parameter

$$\phi_T \equiv \frac{n_{A0} \hat{C}_p}{h} = \frac{w_{A0} \hat{C}_p}{h_m} \quad (56)$$

Here  $h$  and  $h_m$  are the local and mean heat-transfer coefficients, respectively, in the absence of mass transfer, obtainable from equations (47) and (51). Mass transfer into the fluid (positive  $\phi_T$ ) thickens the thermal boundary layer, and

mass transfer out of the fluid makes the boundary layer thinner, just as in forced-convection systems. The velocity gradient at the interface, however, increases with  $\phi_T$ , which is just the opposite of the behavior usually found in forced-convection systems. This behavior is due to the increase in the total buoyant force with increasing thermal boundary-layer thickness.

The momentum and heat transfer rates in the presence of mass transfer are still given by

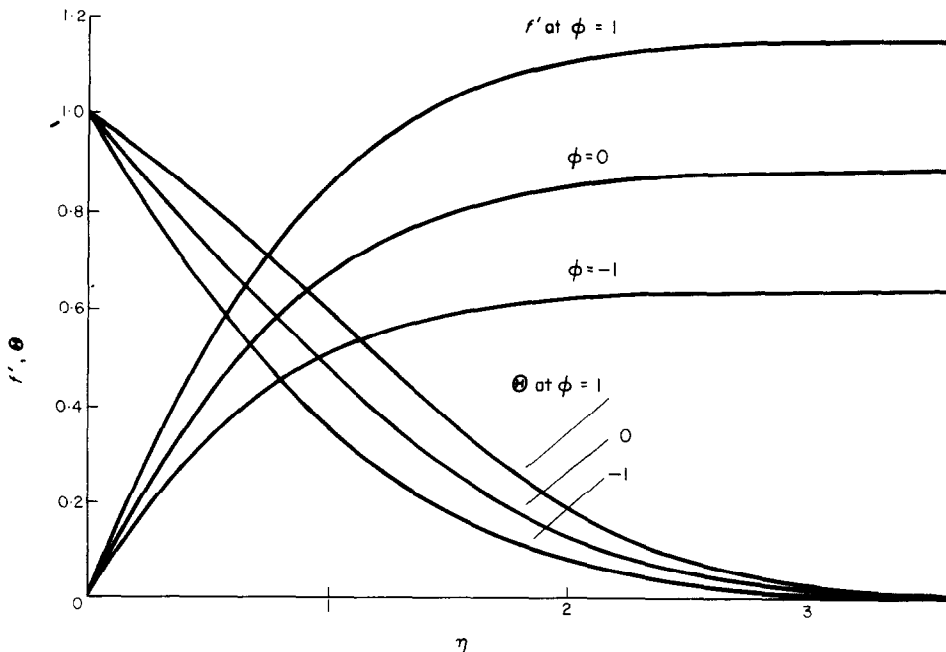


FIG. 3. Boundary-layer profiles at high Prandtl or Schmidt number and various mass-transfer rates.

Table 3. Coefficients for equations (46)–(51) as functions of mass-transfer rate

$\phi$	$-\Theta'(0)$	$R$	$f''(0)$	$\phi$	$-\Theta'(0)$	$R$	$f''(0)$
-0.0	0.5402	-0.0000	1.085	0.0	0.5402	0.0000	1.085
-0.1	0.5671	-0.0953	1.064	0.1	0.5143	0.1051	1.106
-0.2	0.5948	-0.1817	1.044	0.2	0.4892	0.2209	1.126
-0.3	0.6234	-0.2600	1.023	0.3	0.4651	0.3486	1.147
-0.4	0.6530	-0.3311	1.003	0.4	0.4417	0.4893	1.168
-0.5	0.6834	-0.3954	0.983	0.5	0.4193	0.6444	1.188
-0.6	0.7147	-0.4537	0.962	0.6	0.3977	0.8153	1.209
-0.7	0.7469	-0.5064	0.942	0.7	0.3769	1.004	1.230
-0.8	0.7801	-0.5542	0.922	0.8	0.3570	1.211	1.250
-0.9	0.8141	-0.5974	0.903	0.9	0.3378	1.440	1.270
-1.0	0.8489	-0.6366	0.883	1.0	0.3194	1.692	1.291
-1.1	0.8847	-0.6719	0.864	1.1	0.3019	1.969	1.311
-1.2	0.9213	-0.7039	0.845	1.2	0.2850	2.275	1.331
-1.3	0.9587	-0.7328	0.826	1.3	0.2689	2.612	1.351
-1.4	0.9970	-0.7588	0.807	1.4	0.2536	2.984	1.371
-1.5	1.0361	-0.7824	0.789	1.5	0.2389	3.393	1.391
-1.6	1.0759	-0.8036	0.770	1.6	0.2249	3.845	1.411
-1.7	1.1165	-0.8228	0.753	1.7	0.2116	4.343	1.430
-1.8	1.1579	-0.8401	0.735	1.8	0.1989	4.891	1.450
-1.9	1.2000	-0.8557	0.718	1.9	0.1868	5.497	1.469
-2.0	1.2427	-0.8697	0.701	2.0	0.1753	6.164	1.488
-2.5	1.4662	-0.9214	0.622	2.5	0.1263	10.69	1.582
-3.0	1.7030	-0.9520	0.553	3.0	0.0894	18.14	1.671
-4.0	2.2040	-0.9808	0.442	4.0	0.0424	51.02	1.835
$-\infty$	$\infty$	-1.0000	0.000	$\infty$	0.0000	$\infty$	$\infty$

equations (46)–(51), but with altered values of the coefficients  $f''(0)$  and  $\Theta'(0)$ . These values are given in Table 3. The table may be entered with the argument  $\phi_T$  for problems where the mass-transfer rate is known, or with  $R_T$  if the mass-transfer rate is to be found.

HEAT TRANSFER IN POWER-LAW FLUIDS

The foregoing results can be generalized to certain non-Newtonian flows, namely, those in which the stress tensor  $\tau$  is a power function of the rate-of-strain tensor  $\nabla \mathbf{v}$ . For boundary-layer flows, the normal component of  $\nabla \mathbf{v}$  is dominant, and the following expression of the "power law" is adequate:

$$\tau_{yt} = -K \left| \frac{\partial v_t^*}{\partial y^*} \right|^{n-1} \frac{\partial v_t^*}{\partial y^*} \quad (57)$$

Here dimensional quantities are used, so that  $K$  has the usual dimensions.

With this modified stress relation, equation (2)

is replaced by

$$\begin{aligned} & \left[ \frac{\rho \alpha}{K} \left( \frac{l^2}{\alpha} \right)^{n-1} \right]^2 [\mathbf{v} \cdot \nabla \mathbf{v}]_t \\ & = \left[ \frac{\rho \alpha}{K} \left( \frac{l^2}{\alpha} \right)^{n-1} \right] \frac{\partial}{\partial y} \left[ \left| \frac{\partial v_t}{\partial y} \right|^{n-1} \frac{\partial v_t}{\partial y} \right] \\ & - \frac{g_t}{g} \left[ \frac{l^3 \rho^2 g \beta_T (T_0 - T_\infty)}{K^2} \left( \frac{l^2}{\alpha} \right)^{2n-2} \right] \Theta. \end{aligned} \quad (58)$$

The coefficients provide natural generalizations of the Grashof and Prandtl numbers:

$$Gr = \left[ \frac{l^3 \rho^2 g \beta_T (T_0 - T_\infty)}{K^2} \left( \frac{l^2}{\alpha} \right)^{2n-2} \right] \quad (59)$$

$$Pr = \left[ \frac{K}{\rho \alpha} \left( \frac{\alpha}{l^2} \right)^{n-1} \right]. \quad (60)$$

It should be noted that these generalized forms of  $Gr$  and  $Pr$  are specific to the characteristic velocity  $\alpha/l$  used in this paper. Other generalized

forms are available [1], but equations (59) and (60) are the most convenient here.

The solutions for  $n = 1$  given earlier can be extended to all  $n > 0$  by the following substitutions. Equations (13), (15), (23), (34) and (44) are replaced by:

$$\frac{\partial}{\partial y} \left[ \left| \frac{\partial v_t^{(i)}}{\partial y} \right|^{n-1} \frac{\partial v_t^{(i)}}{\partial y} \right] = \frac{g_t}{g} Gr Pr \Theta \quad (61)$$

$$v_t^{(i)} = \frac{-\frac{g_t}{g} Gr Pr}{\left| \frac{g_t}{g} Gr Pr \right|^{1-1/n}} \times \int_0^y \left| \int_{y'}^{\infty} \Theta(x, y'', z) dy'' \right|^{1/n} dy' \quad (62)$$

$$\frac{1}{Gh_z^n} \frac{\partial}{\partial y} \left[ \left| \frac{\partial^2 \psi}{\partial y^2} \right|^{n-1} \frac{\partial^2 \psi}{\partial y^2} \right] = -Gr Pr \Theta \quad (63)$$

$$\left| \frac{\varphi^n}{Gr Pr Gh_z^n} \delta_T^{2n+1} \right| \frac{d}{d\eta} (f'')^n = -\Theta \quad (64)$$

$$\frac{d}{d\eta} \left( \frac{d^2 f}{d\eta^2} \right)^n = -\Theta. \quad (65)$$

Equations (42) and (43) then are replaced by the more general forms:

$$\varphi = Gr Pr \left| Gr Pr \right|^{-\frac{3n}{3n+1}} \times \left| \frac{3n+1}{2n+1} \int_{x_s(z)}^x G^{-\frac{2n}{2n+1}} h_z^{\frac{3n+1}{2n+1}} dx \right|^{\frac{2n+1}{3n+1}} \quad (66)$$

$$\frac{\delta_T}{l} = \left| Gr Pr \right|^{-\frac{1}{3n+1}} \left[ Gh_z^n \right]^{-\frac{1}{2n+1}} \times \left| \frac{3n+1}{2n+1} \int_{x_s(z)}^x G^{-\frac{2n}{2n+1}} h_z^{\frac{3n+1}{2n+1}} dx \right|^{\frac{n}{3n+1}} \quad (67)$$

The rest of equations (1)–(45) remain as written, but with  $Gr$  and  $Pr$  now given by equations (59) and (60).

Equations (65) and (45) can be solved, with the boundary conditions (36)–(40), to obtain

the profiles of  $f$  and  $\Theta$  at any  $n > 0$ . This same set of equations was solved by Acrivos [1] in his treatment of two-dimensional systems. The resulting values of  $[f''(0)]^n$  and  $\Theta'(0)$  are plotted in Figs. 2 and 3 of his paper, and hold directly in three dimensions with the coordinate  $\eta$  now defined by equations (33) and (67).

The interfacial fluxes now are given by:

$$\begin{aligned} \frac{\tau_0}{l \rho g \beta_T (T_0 - T_\infty)} &= G \frac{\delta_T}{l} \int_0^\infty \Theta d\eta \\ &= [f''(0)]^n \left| Gr Pr \right|^{-\frac{1}{3n+1}} \left[ G^2 h_z^{-1} \right]^{\frac{n}{2n+1}} \\ &\times \left| \frac{3n+1}{2n+1} \int_{x_s(z)}^x G^{-\frac{2n}{2n+1}} h_z^{\frac{3n+1}{2n+1}} dx \right|^{\frac{n}{3n+1}} \quad (68) \end{aligned}$$

and:

$$\begin{aligned} \frac{q_0 l}{k(T_0 - T_\infty)} &= -\Theta'(0) \frac{l}{\delta_T} \\ &= -\Theta'(0) \left| Gr Pr \right|^{\frac{1}{3n+1}} \left[ Gh_z^n \right]^{\frac{1}{2n+1}} \\ &\times \left| \frac{3n+1}{2n+1} \int_{x_s(z)}^x G^{-\frac{2n}{2n+1}} h_z^{\frac{3n+1}{2n+1}} dx \right|^{-\frac{n}{3n+1}} \quad (69) \end{aligned}$$

The transfer expressions for the entire surface correspondingly become

$$\frac{F_D}{l^3 \rho g \beta_T (T_0 - T_\infty)} = C_1(n) \left| Gr Pr \right|^{-\frac{1}{3n+1}} \quad (70)$$

and

$$Nu_m = C_2(n) \left| Gr Pr \right|^{\frac{1}{3n+1}} \quad (71)$$

where the coefficients  $C_1(n)$  and  $C_2(n)$  are calculated as follows:

$$C_1(n) = [f''(0)]^n \int_{z_l}^{z_H} \int_{x_s(z)}^{x_f(z)}$$

$$\times \left| \frac{3n+1}{2n+1} \int_{x_s(z)}^x G^{-\frac{2n}{2n+1}} h_z^{\frac{3n+1}{2n+1}} dx_1 \right|^{\frac{n}{3n+1}} \times G^{-\frac{2n+2}{2n+1}} h_z^{\frac{n+1}{2n+1}} |dx dz|. \quad (72)$$

thus becomes:

$$g_{\text{eff}} = g - a + [[\omega \times r] \times \omega]. \quad (75)$$

The terms on the right are the gravitational, translational and centrifugal contributions.

The preceding development can be applied here by substituting  $g_{\text{eff}}$  and  $\hat{\Phi}_{\text{eff}}$  for  $g$  and  $\hat{\Phi}$ .

$$C_2(n) = - \frac{\Theta'(0) \int_{z_I}^{z_H} \left| \frac{3n+1}{2n+1} \int_{x_s(z)}^{x_f(z)} G^{-\frac{2n}{2n+1}} h_z^{\frac{3n+1}{2n+1}} dx \right|^{\frac{2n+1}{3n+1}} |dz|}{\int_{z_I}^{z_H} \int_{x_s(z)}^{x_f(z)} |G^{-1} h_z dx dz|}. \quad (73)$$

The heat-transfer expressions given by Acrivos [1], for two-dimensional and axially symmetric systems, are specializations of equation (69) and (71). A table of  $C_2(n)$  for several shapes is given in his paper.†

ROTATING AND ACCELERATING SYSTEMS

The foregoing treatment holds for systems at rest, or in steady translational motion with respect to a uniform gravitational field. If the system rotates or accelerates, then additional forces are introduced. These effects are important, for example, in free convection in centrifuges or space vehicles.

Suppose that the transfer surface and undisturbed fluid are transported in a container, and rotate with it at constant angular velocity  $\omega$ . In addition, a reference point of the system moves with a steady linear acceleration  $a$ . Then the work required to move a unit mass to a position  $r$  relative to the reference point, in coordinates fixed relative to the container, is:

$$\hat{\Phi}_{\text{eff}} = \int_0^r \{ (-g + a - [[\omega \times r] \times \omega]) \cdot dr \}. \quad (74)$$

The resultant force on a unit mass located at  $r$

and using a datum  $g_{\text{eff}}$  magnitude,  $g_1$ , in place of  $g$ . The surface coordinate  $x$  is now defined as  $\hat{\Phi}_{\text{eff}}/lg_1$ , and the lines of constant  $z$  are drawn in the direction of the surface gradient of  $\hat{\Phi}_{\text{eff}}$ . Equation (17) then is written,

$$h_x = \frac{lg_1}{|\nabla^2 \hat{\Phi}_{\text{eff}}|} = \frac{1}{G(x, z)} \quad (76)$$

and with this generalization the foregoing solutions can be applied directly. The coefficients  $K_1$  and  $K_2$  must, of course, be recalculated, since they now depend on  $a$  and  $\omega$  in addition to the geometry of the system.

BINARY SYSTEMS

The thermal problems solved here have direct analogs for isothermal binary diffusion. The diffusional results are obtainable by the following substitutions (see Nomenclature):

$$\left. \begin{array}{ll} T \rightarrow \omega_A & Nu \rightarrow Nu_\omega \\ \alpha \rightarrow \mathcal{D}_{AB} & \beta_T \rightarrow \beta_{\omega A} \\ k \rightarrow \rho \mathcal{D}_{AB} & \delta_T \rightarrow \delta_\omega \\ q_0 \rightarrow j_{A0} & R_T \rightarrow R_\omega \\ Pr \rightarrow Sc & \phi_T \rightarrow \phi_{AB} \\ Gr \rightarrow Gr_\omega & \end{array} \right\} \quad (77)$$

† For the vertical cone, the  $C$  values in Reference [1] need to be multiplied by  $(\sin \epsilon)^{\frac{1}{3n+1}}$ . The characteristic length used there is the slant height.

The functions  $f$ ,  $\varphi$  and  $\Theta$ , and the coordinate  $\eta$ , will thus be converted directly into the appropriate forms for diffusion. The assumed constancy of  $R_T$  over the system, in equation (52), implies the constancy of  $n_{A0}/n_{B0}$  in the analogous diffusional problem.

#### RANGE OF VALIDITY

This treatment is based on the usual boundary-layer assumption  $\delta_T/l \ll 1$ , or for diffusion,  $\delta_\omega/l \ll 1$ . This assumption is well satisfied in the mean if  $Nu_m > 5$  or  $Nu_{\omega m} > 5$ , in view of equation (50). The choice of an appropriate  $l$  for this criterion is somewhat subjective, but normally the smallest overall dimension of the surface should be used.

The results are most accurate at large Prandtl or Schmidt numbers. For example, limiting-current measurements at  $Sc \sim 1000$  are reproduced within the experimental error (see Table 2). At smaller Prandtl or Schmidt numbers, the predicted transfer rates are somewhat too high (see Table 4); corrections for this are being provided in a separate paper [12].

This analysis is limited to surfaces free of pockets and equipotential planes, because of the assumptions embodied in equation (15). A simpler rule is that the surface must flood completely when liquid is poured on from the top, and must drain completely afterwards.

#### ACKNOWLEDGEMENTS

The author wishes to thank Jan Sørensen and John Taunton for assistance in the computations, and the National Science Foundation for financial support of this work through Grant GK-678X.

#### REFERENCES

1. ANDREAS ACRIVOS, A theoretical analysis of laminar natural convection heat transfer to non-Newtonian fluids, *A.I.Ch.E. Jl* **6**, 584-590 (1960).
2. MILTON VAN DYKE, *Perturbation Methods in Fluid Mechanics*, Chapter 5. Academic Press, New York (1964).
3. K. STEWARTSON and L. T. JONES, The heated vertical plate at high Prandtl number, *J. Aeronaut. Sci.* **24**, 379-380 (1957).
4. G. W. MORGAN and W. H. WARNER, On heat transfer in laminar boundary layers at high Prandtl number, *J. Aeronaut. Sci.* **23**, 937-948 (1956).
5. F. B. HILDEBRAND, *Advanced Calculus for Applications*, Section 6.17. Prentice-Hall, Englewood Cliffs, N.J. (1962).

Table 4. Comparisons with exact calculations for the vertical plate at  $\phi_T = 0$

Pr	Values of $\frac{F_D  GrPr ^{\frac{1}{2}}}{l^3 \rho g \beta_T (T_0 - T_\infty) K_1}$		Values of $\frac{Nu_m  GrPr ^{-\frac{1}{2}}}{K_2}$	
	Exact [11]	Equation (49)	Exact [11]	Equation (51)
1000	1.073	1.085	0.536	0.5402
100	1.048	1.085	0.526	0.5402
10	0.981	1.085	0.500	0.5402
1	0.845	1.085	0.431	0.5402
0.72	0.820	1.085	0.416	0.5402

This treatment normally holds for the entire transfer surface, since the separation locus (if any) lies at the rear of the transfer surface. Thus, the results are more complete than one obtains from a corresponding treatment [13] of forced convection in these geometries. The difference is due to the possibility of adverse pressure gradients in forced convection systems, and their absence in the systems considered here.

6. G. SCHÜTZ, Natural-convection mass-transfer measurements on spheres and horizontal cylinders by an electrochemical method, *Int. J. Heat Mass Transfer* **6**, 873-879 (1963).
7. C. R. WILKE, C. W. TOBIAS and M. EISENBERG, Free-convection mass transfer at vertical electrodes, *Chem. Eng. Prog.* **49**, 663-674 (1953).
8. N. IBL, The use of dimensionless groups in electrochemistry, *Electrochim. Acta* **1**, 117-129 (1959).
9. HOWARD BRENNER, On the invariance of the heat-transfer coefficient to flow reversal in Stokes and

potential streaming flows past particles of arbitrary shape, *J. Math. Phys. Sci.* **1**, 173-179 (1967).

10. R. B. BIRD, W. E. STEWART and E. N. LIGHTFOOT, *Transport Phenomena*, pp. 672-676. John Wiley, New York (1960).
11. SIMON OSTRACH, An analysis of laminar free-convection flow and heat transfer about a flat plate parallel to the direction of the generating body force, NACA Report 1111 (1953).
12. J. W. TAUNTON, E. N. LIGHTFOOT and W. E. STEWART, Simultaneous free-convection heat and mass transfer in laminar boundary layers, *Chem. Engng Sci.* **25**, 1927-1937 (1970).
13. W. E. STEWART, Forced convection in three-dimensional flows: I. Asymptotic solutions for fixed interfaces, *A.I.Ch.E. Jl* **9**, 528-535 (1963).

APPENDIX A

Calculation of  $K_1$  and  $K_2$

A1. The sphere

For this system we take  $l = D$ ,  $x = \frac{1}{2} \cos \theta$  and  $z = \phi$ , where  $\xi = r/D$ , and  $\theta$  and  $\phi$  are the usual spherical angle coordinates. The  $\nabla$  operator in these coordinates is

$$\nabla = \delta_\xi \frac{\partial}{\partial \xi} + \delta_\theta \frac{1}{\xi} \frac{\partial}{\partial \theta} + \delta_\phi \frac{1}{\xi \sin \theta} \frac{\partial}{\partial \phi} \tag{A.1}$$

and its projection on the surface is:

$$\nabla^s = \left[ \delta_\theta \frac{1}{\xi} \frac{\partial}{\partial \theta} + \delta_\phi \frac{1}{\xi \sin \theta} \frac{\partial}{\partial \phi} \right]_{\xi=\frac{1}{2}} \tag{A.2}$$

Hence,

$$G = h_x^{-1} = |\nabla^s x| = |\delta_\theta (-\sin \theta)| = \sin \theta \tag{A.3}$$

$$h_z^{-1} = |\nabla^s z| = \left| \delta_\phi \left( \frac{2}{\sin \theta} \right) \right| = \frac{2}{\sin \theta} \tag{A.4}$$

Equations (49) and (50) can then be applied, with  $x = \frac{1}{2} \cos \theta$ ,  $x_s = -\frac{1}{2}$  and  $x_r = \frac{1}{2}$ , to obtain:

$$\begin{aligned} K_1 &= \int_0^{2\pi} \int_0^\pi \left| \frac{4}{3} \int_\pi^\theta (\sin \theta_1)^{-\frac{1}{2}} \left( \frac{1}{2} \sin \theta_1 \right)^{\frac{1}{2}} \left( -\frac{1}{2} \sin \theta_1 d\theta_1 \right) \right|^{\frac{1}{2}} \\ &\quad \times (\sin \theta)^{-\frac{1}{2}} \left( \frac{1}{2} \sin \theta \right)^{\frac{1}{2}} \times \left( -\frac{1}{2} \sin \theta d\theta \right) d\phi \tag{A.5} \\ &\equiv 3.204 \text{ by numerical integration} \\ K_2 &= \frac{\int_0^{2\pi} \int_0^\pi \left| \frac{4}{3} \int_\pi^\theta (\sin \theta)^{-\frac{1}{2}} \left( \frac{1}{2} \sin \theta \right)^{\frac{1}{2}} \left( -\frac{1}{2} \sin \theta d\theta \right) \right|^{\frac{1}{2}} d\phi}{\int_0^{2\pi} \int_0^\pi \left( \frac{1}{2} \right) \left( -\frac{1}{2} \sin \theta d\theta \right) d\phi} \\ &= \left| \frac{2}{3} B\left(\frac{1}{2}, \frac{3}{2}\right) \right|^{\frac{1}{2}} \equiv 1.090. \tag{A.6} \end{aligned}$$

Here  $B(a, b)$  is the beta function.

A2. The inclined plate

Here we take  $l = L$ ,  $x = X \cos \theta$  and  $z = Z$ , where  $X$  and  $Z$  are dimensionless Cartesian coordinates measured along the slope and width of the plate. Then writing the surface gradient in the coordinates  $X, Z$  we get

$$\nabla^s = [\delta_X \partial / \partial X + \delta_Z \partial / \partial Z]_{y=0} \tag{A.7}$$

and equation (17) and (18) give:

$$G = h_x^{-1} = \cos \theta; \quad h_z = 1. \tag{A.8}$$

Substitution in equations (49) and (50) yields the following results for  $K_1$  and  $K_2$ :

$$\begin{aligned} K_1 &= \int_0^{W/L} \int_0^{\cos \theta} \left| \frac{4}{3} \int_0^x (\cos \theta)^{-\frac{1}{2}} dx_1 \right|^{\frac{1}{2}} (\cos \theta)^{-\frac{1}{2}} dx dz \\ &= \frac{4}{3} \left( \frac{W}{L} \right)^{\frac{1}{2}} (\cos \theta)^{-\frac{1}{2}} \tag{A.9} \end{aligned}$$

$$K_2 = \frac{\int_0^{W/L} \left| \frac{4}{3} \int_0^{\cos \theta} (\cos \theta)^{-\frac{1}{2}} dx \right|^{\frac{1}{2}} dz}{\int_0^{W/L} \int_0^{\cos \theta} (\cos \theta)^{-1} dx dz} = \left( \frac{4}{3} \right)^{\frac{1}{2}} (\cos \theta)^{\frac{1}{2}}. \tag{A.10}$$

These results are valid as long as the plate is not level ( $\cos \theta \neq 0$ ).

A3. The inclined cylinder

This geometry is illustrated in Fig. 4 and Table 1. The transfer zone is of length  $L$  on the cylindrical surface. The remainder of the surface is insulated, and may consist of flat ends as shown, or an extension of the cylindrical surface.

We use dimensionless cylindrical coordinates  $\xi, \theta, \zeta$ , with the cylinder diameter  $D$  as the characteristic length. The dimensionless elevation at any point  $\theta, \zeta$  on the surface  $\xi = \frac{1}{2}$  then becomes:

$$x = -\frac{1}{2} \cos \theta \cos \gamma + \zeta \sin \gamma. \tag{A.11}$$

The surface gradient of  $x$  is

$$\nabla^s x = \left[ \delta_\theta \frac{1}{\xi} \frac{\partial x}{\partial \theta} + \delta_\zeta \frac{\partial x}{\partial \zeta} \right]_{\xi=\frac{1}{2}} = \delta_\theta \sin \theta \cos \gamma + \delta_\zeta \sin \gamma \tag{A.12}$$

and its magnitude is

$$G = h_x^{-1} = \sqrt{[\sin^2 \theta \cos^2 \gamma + \sin^2 \gamma]}. \tag{A.13}$$

The general expression for a differential displacement on the surface is

$$Dds = \delta_\theta \frac{1}{2} D d\theta + \delta_\zeta D d\zeta. \tag{A.14}$$

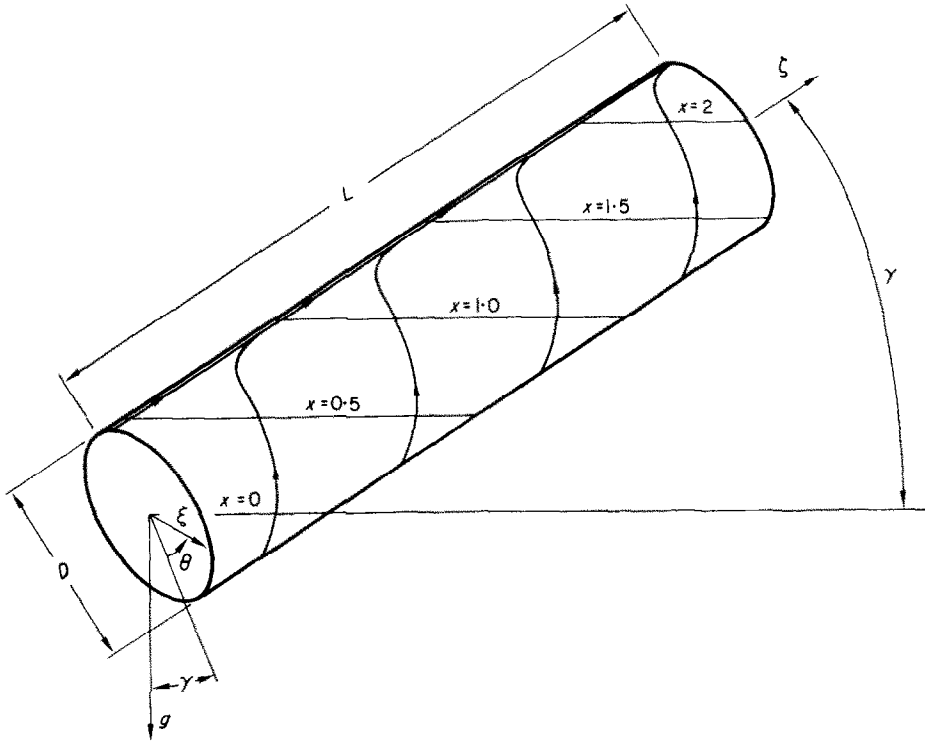


FIG. 4. Horizontal oblique view of tilted cylinder, showing surface coordinate grid. The curved paths are steepest-ascent lines, computed from equation (A.20). The angles between the grid lines are altered by the projection; all are right angles on the surface.

Taking  $ds$  parallel to  $\nabla^2 x$  gives the differential equation for the trajectories of steepest ascent:

$$\frac{d\theta}{2 \sin \theta \cos \gamma} = \frac{d\zeta}{\sin \gamma} \quad (\text{steepest ascent}). \quad (\text{A.15})$$

Integration gives the surface streamlines:

$$\frac{1}{2} \sin \gamma \log \tan \frac{1}{2} \theta = \zeta \cos \gamma + C(z). \quad (\text{A.16})$$

Here  $C(z)$  is a function of integration, which will become definite when  $z$  is defined. The total differential of  $x$  along a surface streamline is found from (A.11) and (A.15):

$$dx = \frac{1}{2} \sin \theta \cos \gamma d\theta + \sin \gamma d\zeta$$

$$= \begin{cases} \frac{\sin^2 \theta \cos^2 \gamma + \sin^2 \gamma}{2 \sin \theta \cos \gamma} d\theta & (\gamma \neq \pi/2) \\ \frac{\sin^2 \theta \cos^2 \gamma + \sin^2 \gamma}{\sin \gamma} d\zeta & (\gamma \neq 0). \end{cases} \quad (\text{A.17})$$

The special case  $\gamma = 0$  will be considered first.

If the cylinder is horizontal ( $\gamma = 0$ ), then the left-hand side of (A.16) vanishes and the surface streamlines are half-circles of constant  $\zeta$ . The choice  $z = \zeta$  is then convenient; this gives  $h_z = 1$  and leads to the following evaluation of  $K_1$  and  $K_2$ :

$$K_1 = 2 \int_0^{L/D} \int_0^{\pi} \left| \frac{1}{3} \int_0^{\pi} (\sin \theta_1)^{-\frac{1}{3}} (\frac{1}{2} \sin \theta_1 d\theta_1) \right|^{\frac{2}{3}} \times (\sin \theta)^{-\frac{1}{3}} (\frac{1}{2} \sin \theta d\theta) d\zeta$$

$$\doteq 3.612 L/D \text{ by numerical integration (horizontal) (A.18)}$$

$$K_2 = \frac{\int_0^{L/D} \left| \frac{1}{3} \int_0^{\pi} (\sin \theta)^{-\frac{1}{3}} (\frac{1}{2} \sin \theta d\theta) \right|^{\frac{2}{3}} d\zeta}{\int_0^{L/D} \int_0^{\pi} (\sin \theta)^{-1} (\frac{1}{2} \sin \theta d\theta) d\zeta}$$

$$= \frac{2}{\pi} \left[ \frac{2}{3} B \left( \frac{1}{2}, \frac{2}{3} \right) \right]^{\frac{2}{3}} \doteq 0.9581 \quad (\text{horizontal}). \quad (\text{A.19})$$



The factor of 2 in front of the integral for  $K_1$  is needed to include both sides of the cylinder, for this choice of  $z$ .

If the cylinder is not horizontal, then each surface streamline passes through the plane  $\zeta = 0$ , and we may define  $z$  as the value of  $\theta$  on the streamline at that intersection. Equation (A.16) then becomes:

$$\log \tan \frac{1}{2} \theta - \log \tan \frac{1}{2} z = 2\zeta \cot \gamma. \quad (\text{A.20})$$

The surface gradient of this  $z$ -coordinate is  $\nabla^s z = [\nabla^s \log \tan \frac{1}{2} z] (dz/d \log \tan \frac{1}{2} z)$

$$= [\delta_\theta(2/\sin \theta) - \delta_\zeta(2 \cot \gamma)] (\sin z) \quad (\text{A.21})$$

and its magnitude is:

$$h_z^{-1} = \sqrt{[\sin^2 \gamma + \sin^2 \theta \cos^2 \gamma]} (2 \sin z / \sin \gamma \sin \theta) \quad (\text{A.22})$$

Insertion of equations (A.13), (A.17) and (A.22) into (49) and (50), and integration over the surface of the cylinder ( $-\pi < z < \pi$ ,  $0 < \zeta < L/D$ ), gives for  $\gamma \neq 0$ :

$$K_1 = \int_{-\pi}^{\pi} \int_0^{L/D} \left| \frac{4}{3} \int_0^{\zeta} \left( \frac{\sin \gamma \sin \theta_1}{2 \sin z} \right)^{\frac{4}{3}} \frac{d\zeta_1}{\sin \gamma} \right|^{\frac{4}{3}} \times \left( \frac{\sin \gamma \sin \theta}{2 \sin z} \right)^{\frac{4}{3}} \frac{d\zeta dz}{\sin \gamma} \quad (\text{A.23})$$

$$K_2 = \frac{\int_{-\pi}^{\pi} \int_0^{L/D} \left| \frac{4}{3} \int_0^{\zeta} \left( \frac{\sin \gamma \sin \theta}{2 \sin z} \right)^{\frac{4}{3}} \frac{d\zeta}{\sin \gamma} \right|^{\frac{4}{3}} dz}{\int_{-\pi}^{\pi} \int_0^{L/D} \frac{\sin \theta}{2 \sin z} d\zeta dz} \quad (\text{A.24})$$

These expressions can be simplified by use of the following rearrangement of equation (A.20):

$$\frac{\sin \theta}{\sin z} = \left[ \frac{\cot^2 \frac{1}{2} z + 1}{\cot^2 \frac{1}{2} z + e^{4u}} \right] e^{2u} = F(z, u) \quad (\text{A.25})$$

where

$$u = \zeta \cot \gamma. \quad (\text{A.26})$$

The results for  $K_1$  and  $K_2$  then become:

$$K_1 = (\sin \gamma)^{-\frac{4}{3}} (\cot \gamma)^{-\frac{4}{3}} \int_0^{\pi} \int_0^{(L/D)\cot \gamma} \left| \frac{4}{3} \int_0^u F^{\frac{4}{3}}(z, u_1) du_1 \right|^{\frac{4}{3}} F^{\frac{4}{3}}(z, u) du dz \quad (\text{A.27})$$

$$K_2 = \frac{(\sin \gamma)^{\frac{4}{3}} (\cot \gamma)^{-\frac{4}{3}} \int_0^{\pi} \int_0^{(L/D)\cot \gamma} F^{\frac{4}{3}}(z, u) du}{\pi(L/D)} dz. \quad (\text{A.28})$$

In the limit as  $(L/D) \cot \gamma$  approaches zero, the function  $F(z, u)$  becomes equal to unity on the entire surface, and equations (A.27) and (A.28) can be integrated analytically to obtain:

$$K_1 \rightarrow (\sin \gamma)^{-\frac{4}{3}} \pi \left( \frac{4}{3} \right)^{\frac{4}{3}} \left( \frac{L}{D} \right)^{\frac{4}{3}} \left( \frac{L}{D} \cot \gamma \rightarrow 0 \right) \quad (\text{A.29})$$

$$K_2 \rightarrow (\sin \gamma)^{\frac{4}{3}} \left( \frac{4}{3} \right)^{\frac{4}{3}} \left( \frac{L}{D} \right)^{-\frac{4}{3}} \left( \frac{L}{D} \cot \gamma \rightarrow 0 \right). \quad (\text{A.30})$$

These results hold for very short inclined cylinders, as well as for nearly vertical cylinders.

For large values of  $\cot \gamma$ , i.e. nearly horizontal cylinders, the limit of equations (A.18) and (A.19) is approached. A more detailed calculation, using the full equation (A.16) and the form of (A.17) valid for  $\gamma \neq \pi/2$ , gives:

$$K_1 \rightarrow 3.612 (L/D) (\cos \gamma)^{-\frac{4}{3}} \left( \frac{L}{D} \cot \gamma \rightarrow \infty \right) \quad (\text{A.31})$$

$$K_2 \rightarrow 0.9581 (\cos \gamma)^{\frac{4}{3}} \left( \frac{L}{D} \cot \gamma \rightarrow \infty \right). \quad (\text{A.32})$$

These forms are valid for very long cylinders, as well as for nearly horizontal ones.

At intermediate values of  $(L/D) \cot \gamma$ , numerical integration is required. A short list of values is given in Table 1.

A4. The isothermal disk fin

The isothermal (perfectly conducting) disk fin is studied here as a limiting case of actual fins. The geometry is illustrated in Table 1 and Fig. 5. Rectangular coordinates are used, with  $l = D_f$ ,  $h_x = 1$  and (since the areas considered are vertical)  $h_z = 1$ . The fin and tube surfaces are assumed to join squarely (no fillet). With this type of joint, the boundary layers on the fin and tube are independent in the high-Pr limit, and equations (A.18) and (A.19) hold for the tube.

The boundaries of the fin are

$$x^2 + z^2 = \frac{1}{4} B^2 \quad (\text{Joint}) \quad (\text{A.33})$$

and

$$x^2 + z^2 = \frac{1}{4} \quad (\text{Outer Edge}) \quad (\text{A.34})$$

where  $B = D_T/D_f$ . These expressions provide the loci  $x_s(z)$  and  $x_f(z)$ . Thus, for Regions A1 and A2 of Fig. 5,  $x_s = -\sqrt{(\frac{1}{4} - z^2)}$  and  $x_f = +\sqrt{(\frac{1}{4} - z^2)}$ , whereas for B1 and B2,  $x_s = +\sqrt{(\frac{1}{4} B^2 - z^2)}$  and  $x_f = +\sqrt{(\frac{1}{4} - z^2)}$ . Note that the upper half of the joint forms the stagnation locus for B1 and B2, since it is the bottom terminus of the steepest ascent paths for B1 and B2 as long as the joint is square. If the joint were filleted, then fluid could move across it by steepest ascent from the surface of the tube; in that case the

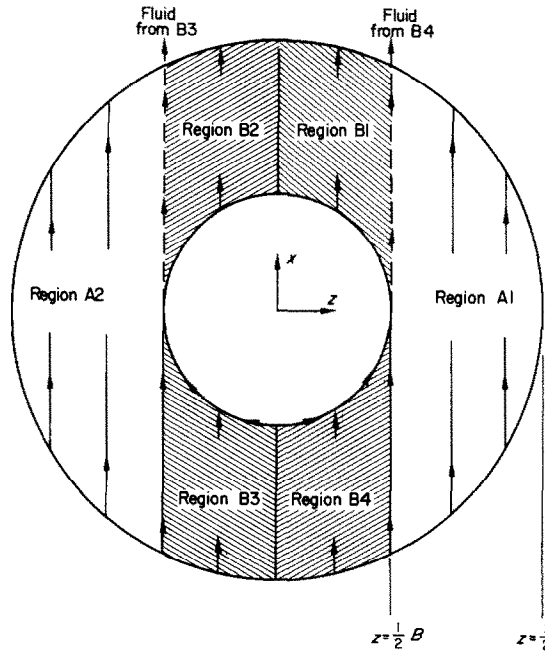


FIG. 5. Flow paths and integration regions for the disk fin on a horizontal tube. The arrows show the local direction of steepest ascent.

joint would not be a stagnation locus, and the total heat transfer rate would be reduced.

In Regions B3 and B4, the streamlines rise vertically from  $x_s = -\sqrt{(\frac{1}{4} - z^2)}$  up to the joint. They run together at the joint and flow along it until it becomes vertical; then they peel off and rise straight to the top of the fin in accordance with the steepest ascent rule. For these streamlines, the value of  $x_f$  is  $\sqrt{(\frac{1}{4} - \frac{1}{2} B^2)}$ ; however, the contributions to  $K_1$  and  $K_2$  come entirely from the shaded areas below the tube, since the "piling up" of the boundary layer at the joint reduces its width to zero from there on.

This "piling up" of the boundary layer from B3 and B4 is an exaggeration of the actual physical situation, and is caused by the boundary-layer approximations used here. It should not be taken literally but as a simplified description of a region that contributes little to the total transfer rates. Comparable situations occur at the separation locus on the cylinder and sphere, without significant effect on the predictions of  $Nu_m$  at high  $Pr$  or  $Sc$ ; see Table 1.

With these specifications, equations (49) and (50) give:

$$\begin{aligned}
 K_1 &= 8 \int_0^{\frac{1}{2}B} \int_{\sqrt{(\frac{1}{4}B^2 - z^2)}}^{\sqrt{(\frac{1}{4} - z^2)}} \left| \frac{4}{3} [x - \sqrt{(\frac{1}{4}B^2 - z^2)}] \right|^{\frac{1}{2}} dx dz \\
 &+ 4 \int_{\frac{1}{2}B}^{\frac{1}{2}} \int_{-\sqrt{(\frac{1}{4} - z^2)}}^{\sqrt{(\frac{1}{4} - z^2)}} \left| \frac{4}{3} [x + \sqrt{(\frac{1}{4} - z^2)}] \right|^{\frac{1}{2}} dx dz \\
 &= 8 \left(\frac{4}{3}\right)^{\frac{1}{2}} \int_0^{\frac{1}{2}B} \left[ \frac{4}{3} \left[ \sqrt{(\frac{1}{4} - z^2)} - \sqrt{(\frac{1}{4}B^2 - z^2)} \right]^{\frac{3}{2}} dz \right. \\
 &\quad \left. + 4 \left(\frac{4}{3}\right)^{\frac{1}{2}} \int_{\frac{1}{2}B}^{\frac{1}{2}} \left[ \frac{4}{3} \left[ 2\sqrt{(\frac{1}{4} - z^2)} \right]^{\frac{3}{2}} dz \right] \right. \quad (A.35)
 \end{aligned}$$

and

$$K_2 = \frac{8 \int_0^{\frac{1}{2}B} \left[ \frac{4}{3} \left[ \sqrt{(\frac{1}{4} - z^2)} - \sqrt{(\frac{1}{4}B^2 - z^2)} \right] \right]^{\frac{1}{2}} dz}{2\pi(\frac{1}{4} - \frac{1}{4}B^2)}$$

$$+ \frac{4 \int_{\frac{1}{2}B}^{\frac{1}{2}} \left| \frac{8}{3} \sqrt{\left(\frac{1}{4} - z^2\right)} \right|^{\frac{1}{2}} dz}{2\pi\left(\frac{1}{4} - \frac{1}{4}B^2\right)}. \quad (\text{A.36})$$

Numerical results are given in Table 1. The total transfer rates correspond to eight times the contribution of Region B1, plus four times that of A1. The results for square fins in Table 1 were obtained analogously.

The performance of non-isothermal fins may be estimated by conventional methods, using a value of  $h_m$  calculated

from equation (51) at a mean temperature difference for the system. This extrapolation of results derived for isothermal surfaces appears to be reasonable, in view of the insensitivity of  $\delta_T$  to position and temperature difference, shown in equation (43).

For multiple fins, the results in Table 1 should be accurate, as long as the thermal boundary layers from adjacent fins do not overlap. On the basis of Fig. 2, no significant overlap is expected at fin spacings more than eight times the mean thermal boundary layer thickness,  $k/h_m$ .

#### CALCUL ASYMPTOTIQUE D'UNE CONVECTION LIBRE DANS DES SYSTÈMES LAMINAIRES TRIDIMENSIONNELS

**Résumé**—Sont données, pour une convection naturelle dans des systèmes laminaires tridimensionnels, des solutions de couche limite établies pour une densité dépendant de la température ou dépendant de la composition. Des effets de transfert de masse rapide et de forces centrifuges sont déterminés et les résultats d'Acrivos (1) pour des fluides à "loi-puissance" sont généralisés. Les résultats sont valables asymptotiquement pour des nombres de Prandtl ou de Schmidt élevés. Ils sont remarquablement bien confirmés par les mesures antérieures sur des réactions électrochimiques limitées par la diffusion.

#### ASYMPTOTISCHE BERECHNUNG DER FREIEN KONVEKTION IN LAMINAREN DREIDIMENSIONALEN SYSTEMEN

**Zusammenfassung**—Es werden Lösungen der Grenzschichtgleichungen angegeben für die freie Konvektion in laminaren dreidimensionalen Systemen. Die Konvektion kann durch Temperatur- bzw. Konzentrationsabhängigkeit der Dichte hervorgerufen sein. Die Einflüsse von raschem Stoffübergang und von Zentrifugalkräften werden bestimmt, und die Ergebnisse von Acrivos [1] für Fluide, die einem Potenzgesetz gehorchen, werden verallgemeinert. Die Ergebnisse gelten asymptotisch für grosse Prandtl- und Schmidtzahlen; sie werden sehr gut bestätigt durch vorangegangene Messungen an diffusionsbegrenzten elektrochemischen Reaktionen.

#### АСИМПТОТИЧЕСКИЙ РАСЧЕТ СВОБОДНОЙ КОНВЕКЦИИ В ЛАМИНАРНЫХ ТРЕХМЕРНЫХ СИСТЕМАХ

**Аннотация**—Приводятся решения уравнений пограничного слоя при свободной конвекции в ламинарных трехмерных системах, обусловленной зависимостью плотности от температуры или состава. Определяются эффекты быстрого массопереноса и центробежных сил. Обобщаются результаты Акривоса для степенных жидкостей. Результаты асимптотически справедливы для больших чисел Прандтля или Шмидта. Они непосредственно подтверждаются предыдущими измерениями электрохимических реакций, контролируемых диффузией.